Journal of The Electrochemical Society, **147** (3) 869-873 (2000)
S0013-4651(99)04-108-5 CCC: $7.00 © The Electrochemical Society, Inc.

In Situ X-Ray Absorption and Diffraction Study of the Li Reaction with a Tin Composite Oxide Glass

A. N. Mansour,[a,*,z] S. Mukerjee[b,*] X. Q. Yang,[c,*] and J. McBreen[c,*]

[a]*Naval Surface Warfare Center, Carderock Division, West Bethesda, Maryland 20817-5700, USA*
[b]*Department of Chemistry, Northeastern University, Boston, Massachusetts 02115, USA*
[c]*Brookhaven National Laboratory, Department of Applied Science, Upton, New York 11973, USA*

We have measured the X-ray absorption fine structure spectra of a sample of tin-based composite oxide (TCO) material with a nominal composition of $Sn_{1.0}B_{0.56}P_{0.40}Al_{0.42}O_{3.47}$ during the discharge and charge cycles in an *in situ* configuration. Our results confirm the amorphous nature of TCO material and show that Sn in the pristine state of TCO is coordinated with three oxygen atoms at a distance of 2.12 Å. Upon discharging, initially Li interacts with the electrochemically active Sn-O center, forming metallic Sn in a highly dispersed form (*i.e.*, clusters containing just a few atoms). Upon further discharge, Li alloys with Sn, forming highly dispersed forms of Li_xSn alloys with x being dependent on the degree of Li intercalation. The structural nature of the highly dispersed alloys differs from those of the corresponding crystalline phases such as Li_2Sn_5, LiSn, Li_7Sn_3, Li_5Sn_2, $Li_{13}Sn_5$, and Li_7Sn_2. Upon charging, Li dealloys from Li_xSn, forming metallic Sn in a highly dispersed form with a Sn-Sn distance intermediate to those of gray and white Sn.

Manuscript submitted April 27, 1999; revised manuscript received October 7, 1999.

Currently, Li-ion rechargeable batteries employ $LiCoO_2$ as a cathode material and a carbon-based intercalation compound such as LiC_6 as an anode material. The LiC_6 anode material, however, has a capacity limited to the theoretical value of 370 mAh/g and suffers from a significant irreversible loss in capacity after only one cycle. Due to these issues, safety concerns, and requirements for higher energy densities, there is a need to look for alternatives to carbon-based materials. Recently, a new class of anode material based on a tin composite oxide (TCO) glass has been proposed as an alternative.[1] TCO material has significantly higher reversible gravimetric (>600 mAh/g) and volumetric (>2200 mAh/cm^3) capacities as compared to carbon-based material. The Sn-based composite oxide, which consists of Sn, B, P, Al, and O, is a very promising anode material when coupled with Li-intercalated cathode materials such as $LiCoO_2$. Results on analogous Sn compounds such as SnO, SnO_2, and Sn_2BPO_6 glass by Courtney and Dahn[2,3] report initial formation of Sn and Li_2O and then Li_xSn alloy phases during the first discharge. Subsequent charge results in formation of Sn aggregates with the formation of Li_2O phase being irreversible. Further cycling has been shown to be a process involving the alloying and dealloying of the various Li_xSn_y phases with irreversibility based on cutoff voltages and size of the Sn aggregates. These observations are in contrast to those suggested by Idota *et al.*,[1] who ascribes an intercalation mechanism for the interaction of Li with the glassy tin composite oxides. In another study,[4] the electrochemical behavior, the effect of composition on cycle life, as well as the Li storage mechanism for a family of $SnB_xP_yO_z$ oxides were investigated. Furthermore, the charge-discharge performance of electron-beam-deposited tin oxide thin-film electrodes was investigated.[5] In this study, the effects of heat-treatment on morphology, structure, and electrochemical performance were examined.

To date, the reaction mechanism of Li with TCO material is not yet fully understood and needs clarification. Part of the problem in deducing a proper mechanistic picture of the interaction of Li with these materials is due to the fine aggregates of different phases formed. X-ray diffraction (XRD) analysis provides minimal structural information due to the amorphous nature of TCO material in the pristine state as demonstrated by Idota *et al.*[1] In addition, we show here that XRD provides minimal structural information even for charged and discharged TCO electrodes due to the formation of fine aggregates. Other techniques, such as Sn^{119} Mössbauer, Li^6 and Li^7 NMR, etc., have limitations on elucidating changes in the *in situ* short-range atomic order around Sn during the charge and discharge reactions. However, x-ray absorption spectroscopy (XAS) is uniquely suited for the elucidation of the structure and composition of amorphous materials, with its *in situ* capability, element specificity, and ability to monitor changes in the local environment of the absorbing atom. Hence, XAS has been used to determine changes in the local atomic structure of Sn during the discharge (*i.e.*, Li insertion) and charge (*i.e.*, Li removal) cycles in an *in situ* configuration. The XAS measurements were made over the intercalation range, which corresponds to a Li/Sn mole ratio of 0-5.4.

Experimental

Sample preparation.—The TCO material with a nominal composition of $Sn_{1.0}B_{0.56}P_{0.40}Al_{0.42}O_{3.47}$ was prepared following the procedure described by Idota *et al.*[1,6] Briefly, the material was prepared by thoroughly mixing appropriate fractions of research-grade SnO, $Sn_2P_2O_7$, B_2O_3, and Al_2O_3 with the aid of acetone. The dried mixture was then placed in an alumina crucible and heated to 1100°C at a rate of 3°C/min to invoke the reaction in the molten state. The sample was then held at 1100°C for 15 h and cooled to room temperature at a rate of 10°C/min. The heating was conducted in a mullite tube furnace with Ar gas flowing. The final product, which is yellowish in color, was characterized by XRD. Its XRD pattern shows an amorphous band similar to that published by Idota *et al.*[1]

Electrochemical measurements.—The electrodes were prepared after sieving the finely ground powder of the material (635 mesh, ~20 μm). Methodology for preparation of the electrodes involved depositing a uniform layer of a slurry comprised of ~80% TCO + 10% acetylene black +10% polyvinylidine fluoride binder using a fugative solvent such as 1-methyl-2-pyrrolidone on a Cu substrate (25 μm thick). This electrode was dried for 3-4 h in a vacuum oven at ~80°C. The electrode loading in terms of TCO material was ~35 mg/cm^2, a weight calculated to give an X-ray absorption step height of 1 ($\Delta\mu x = 1$). The TCO electrode was assembled in a special spectroelectrochemical cell with a 0.8 mm thick Li foil (Aldrich) electrode, which served both as the counter as well as the reference electrode and a commercial separator (Celgard). The electrolyte of choice was ethylene carbonate (EC) + propylene carbonate (PC) + dimethylene carbonate (DMC) in the ratio 1:1:3 with 1 M $LiPF_6$ as the salt. The cell construction allowed for Mylar windows on both end plates to allow XAS spectra to be collected in the transmission mode in order for the bulk of the electrode material to be probed. Details of the cell construction and layout are given elsewhere.[7] Electrochemical charge/discharge was performed between 2.5 and

* Electrochemical Society Active Member.
z E-mail: MansourAN@nswccd.navy.mil

S0013-4651(99)04-108-5 CCC: $7.00

0.14 V *vs.* Li/Li^+ at a rate of 35.6 mA/g TCO using a computer-controlled battery cycler.

XAS measurements.—The XAS experiments were performed on beamline X-11A of the National Synchrotron Light Source with the electron storage ring operating at an electron energy of 2.8 GeV and stored current in the range 110-250 mA. Data were collected with a variable exit double-crystal monochromator using two flat Si(311) crystals. The incident and transmitted X-ray intensities were monitored using ionization chambers (30 cm in length) filled with argon gas. The XAS measurements were continuously collected during both the discharge and charge cycles. The change in the Li/Sn ratio between successive scans was kept near 0.07 to minimize changes in the electrode structure within a single scan. The X-ray absorption edge jump for this electrode was near 0.9 at the Sn K-edge energy (29,200 eV). The XAS measurements were made at room temperature. The number of spectra collected was 63 during the discharge cycle and 36 during the charge cycle. A 50 μm thick white Sn foil was used as a reference for energy calibration and subsequent data analysis.

Quantitative analysis of extended X-ray absortpion fine structure (EXAFS) spectra was made using theoretical standards generated with the FEFF code (version 6.01)[8] employing structural data for crystalline SnO and metallic white Sn. The many body amplitude reduction factor, S_o^2, was determined to be equal to 1.0 (±0.1) from X-ray absorption fine structure (XAFS) data of metallic white Sn. Coordination numbers, bond lengths, and disorders were extracted using nonlinear least-squares fitting procedures in r-space. The fits were made using the curve-fitting code FEFFIT of the UWXAFS package.[9] A single-shell fit of Sn-O bonds was sufficient to fit the data with a Li/Sn ratio in the range 0.0-0.8. A two-shell fit with Sn-O and Sn-Sn bonds was sufficient to analyze the data with a Li/Sn ratio in the range 0.9-1.9. A single-shell fit with Sn-Sn bonds was sufficient to analyze the data with a Li/Sn ratio in the range 2.0-5.4. In all fits, Gaussian pair distribution functions (PDF) for the Sn-O and the Sn-Sn pairs were sufficient to model the EXAFS spectra. The EXAFS spectra for the highly dispersed Sn aggregates were also analyzed using asymmetrical PDF by including the third and fourth terms in the cumulant expansion as fitting parameter. Upon using the asymmetric PDF, the coordination numbers and disorders on the average increased by 17 ± 8% and 30 ± 13%, respectively, relative to those obtained using a Gaussian PDF. The observed increases in the coordination numbers and disorders are random in nature and showed no specific correlation with the Li/Sn ratio. On the average, the Sn-Sn distance increased by 0.030 ± 0.009 Å relative to those obtained assuming a Gaussian PDF. The uncertainties here are given as the standard deviations in the results for the corresponding values of various Li/Sn ratios. For a Li/Sn ratio of 2.44, the coordination number, disorder, and distance increased by 24%, 42%, and 0.023 Å, respectively, relative to those obtained using a Gaussian PDF. The values for the third and fourth terms of the cumulant expansion are 0.00029 ± 0.00018 $Å^3$ and 0.000103 ± 0.00044 $Å,^4$ respectively. For a Li/Sn ratio of 4.76, the coordination number, disorder, and distance increased by 5%, 9%, and 0.030 Å, respectively, relative to those obtained using a Gaussian PDF. The values for the third and fourth terms of the cumulant expansion in this case are 0.00039 ± 0.00020 $Å^3$ and 0.000026 ± 0.000049 $Å,^4$ respectively. Therefore, the effect of asymmetry on the coordination number, disorder, and distance is mild. Hence, hereafter the results obtained using a Gaussian PDF are reported and discussed.

XRD measurements.—The XRD experiments were performed on beamline X-18A of the National Synchrotron Light Source. The data were collected in the transmission mode using X-rays with a wavelength (λ) of 1.195 Å. The geometry of the diffractometer is that of a four-circle Huber diffractometer. The diffracted beam was monitored using a scintillation counter in 2θ steps of 0.02°.

Results

The discharge and charge curves for a typical TCO electrode in a nonaqueous cell is shown in Fig. 1. The voltage profiles for the discharge curve can be described on the basis of three primary regions. Region I displays a voltage plateau near 1.45 V for a Li/Sn ratio in the range 0-1.6, followed by a slow phase transition in region II for a Li/Sn ratio in the range 1.6-3. Region III displays a voltage plateau near 0.16 V for a Li/Sn ratio in the range 3-5.4. In contrast to this, the charge curve showed only two distinct regions corresponding to changes in the Li/Sn ratio of 5.4-3.0 and 3.0-2.3. The large irreversibility in the first cycle, corresponding to recovery of approximately 60% of the discharge capacity, indicates the formation of irreversible phases during the initial Li insertion step. *In situ* XAS spectroscopy and XRD were used to understand the nature of these phase transitions.

In Fig. 2 we show a representative set of Fourier transforms (FTs) of the Sn K-edge EXAFS spectra taken during the discharge cycle (*i.e.*, Li insertion) of a TCO electrode as a function of the Li/Sn ratio, along with that of a control TCO material. The FT for the control TCO material displays a single peak, which corresponds to a Sn-O pair, with no contributions from higher coordination spheres, con-

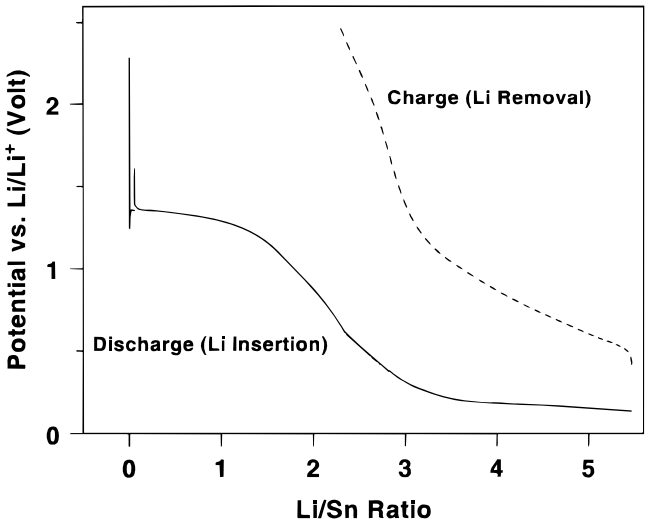

Figure 1. Discharge (Li insertion) and charge (Li removal) profiles for a TCO electrode. The discharge process was interrupted momentarily to realign the cell for the XAFS measurements, hence, the discontinuity observed at the beginning of the discharge cycle.

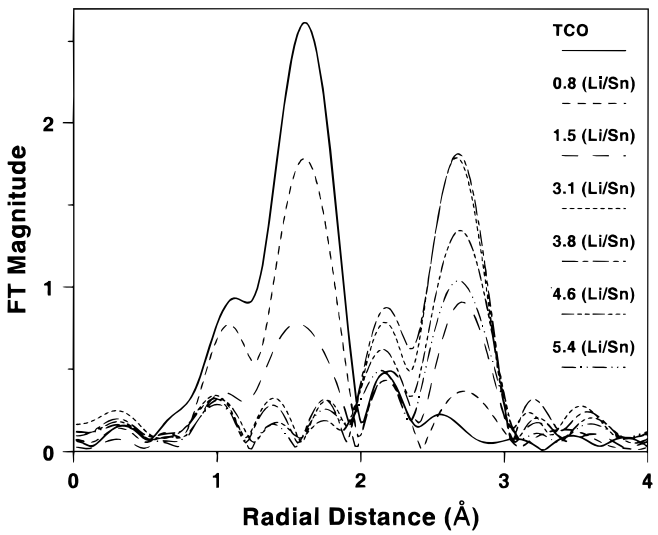

Figure 2. FTs of the k^3 = weighted Sn K-edge EXAFS taken during the discharge cycle as a function of the Li/Sn ratio. FT range is 2.2-11.8 $Å^{-1}$.

S0013-4651(99)04-108-5 CCC: $7.00

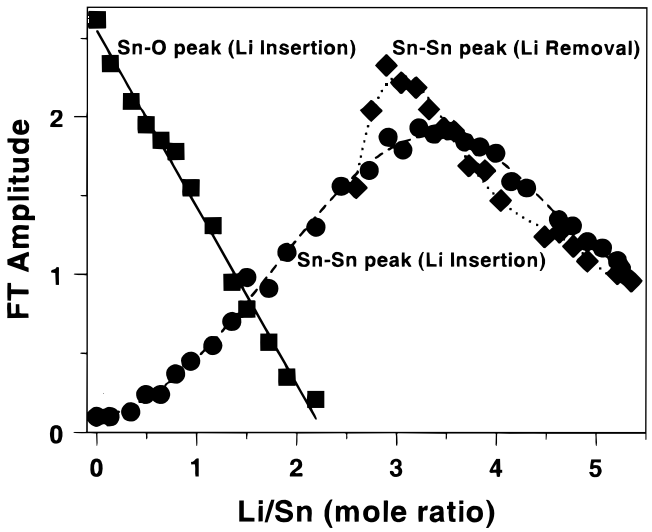

Figure 3. Variations in the amplitude of the FTs as a function of the Li/Sn ratio for the Sn-O peak (during Li insertion) and Sn-Sn peak (during Li insertion and removal).

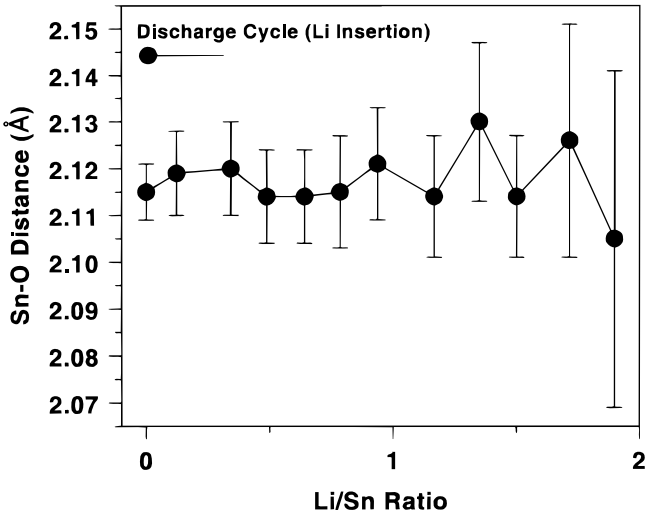

Figure 5. Variations in the Sn-O distance for a TCO electrode as a function of the Li/Sn ratio during the Li insertion process.

firming the amorphous nature of TCO material. As TCO is being discharged, the amplitude of this peak decreases with increases in the value of the Li/Sn ratio and diminishes to a negligible level when the Li/Sn ratio approaches 2.0 (see Fig. 3). A second peak, which corresponds to a Sn-Sn pair, emerges near a Li/Sn ratio of 0.6. The amplitude of this Sn-Sn contribution increases with increases in the Li/Sn ratio up to a value near 3.5. Upon further discharge, the amplitude of this Sn-Sn peak decreases with increases in the value of the Li/Sn ratio up to 5.4.

In Fig. 4 we show a representative set of FTs of the Sn K-edge EXAFS spectra taken during the charge cycle (*i.e.*, Li removal) as a function of the Li/Sn ratio, along with those of control TCO and white metallic Sn. Clearly, the FT data for the charged electrode display a single peak, which corresponds to a Sn-Sn pair. The amplitude of this peak increased with a decrease in the value of the Li/Sn ratio from 5.4 to 2.9 and then decreased with further decreases in the value of the Li/Sn ratio down to 2.6 (see Fig. 3). In addition, the observed Sn-Sn distance for charged TCO is somewhat shorter than that for metallic white Sn. Furthermore, the FT data show the absence of any Sn-O contribution upon Li removal, indicating that the local structure of Sn in the pristine state of TCO has been irreversibly altered.

Local structure parameters such as bond length, coordination number, and disorder for Sn are summarized in Fig. 5, 6, 7, and 8, respectively. The data are shown as a function of the Li/Sn ratio for XAFS spectra taken during the discharge and charge cycles. Only data for every other scan were included in these figures. We show that in the pristine state, Sn in TCO is coordinated with 3.3 oxygen atoms at a distance of 2.12 Å compared to 4 at 2.22 Å in crystalline SnO. Analysis of the X-ray absorption near edge structure (XANES) data show that the oxidation state of Sn in TCO is similar to that of Sn in SnO. [11] Upon discharge, the Sn-O distance remained constant (Fig. 5) while the observed coordination number decreased with increases in the value of the Li/Sn ratio (Fig. 7). The observed coordination number for the Sn-O pair represents the product of the true coordination number (*i.e.*, coordination number in the pristine state, which is equal to 3.3) and the mole fraction of Sn, which is still being coordinated with oxygen. Thus, the apparent decrease in the observed coordination number for the Sn-O pair is due to a decrease in the mole fraction of Sn being coordinated with oxygen. The decrease in the mole fraction of oxidized Sn is consistent with the reaction of Li with the electrochemically active Sn-O center forming

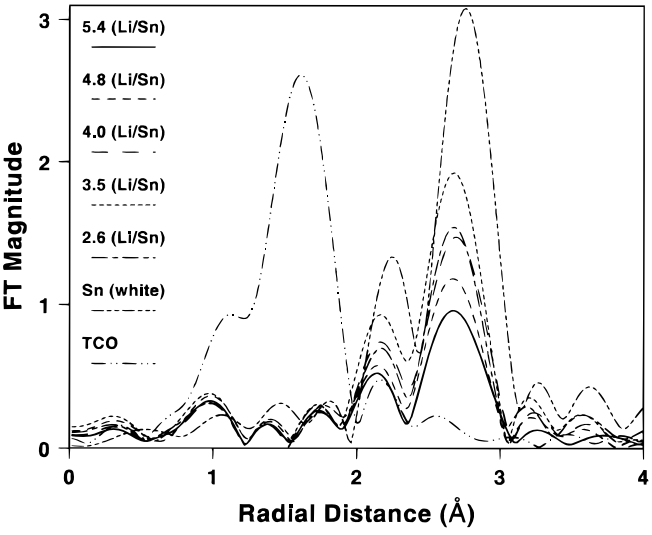

Figure 4. FTs of the k^3 = weighted Sn K-edge EXAFS taken during the charge cycle as a function of the Li/Sn ratio. FT range is 2.2-11.8 $Å^{-1}$.

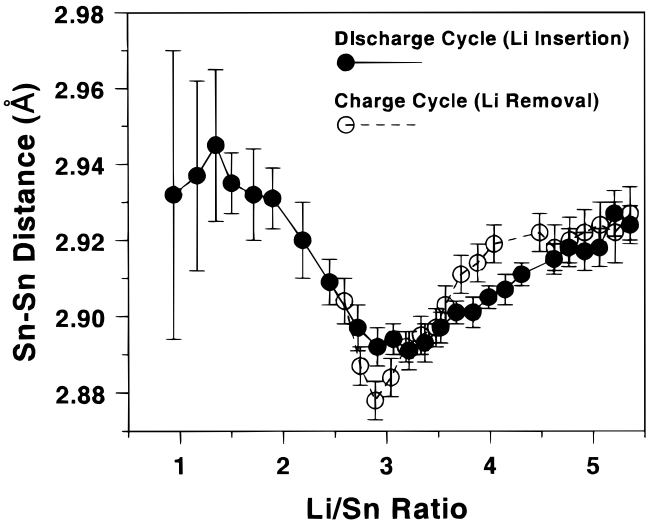

Figure 6. Variations in the Sn-Sn distance for a TCO electrode as a function of the Li/Sn ratio during the Li insertion and removal processes.

S0013-4651(99)04-108-5 CCC: $7.00

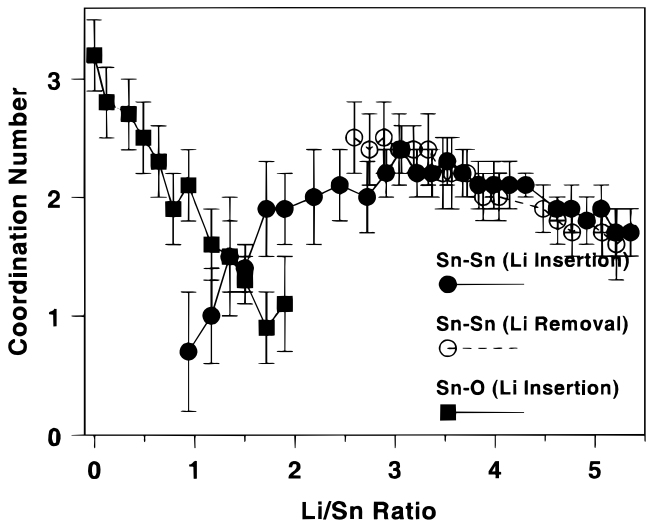

Figure 7. Variations in the coordination numbers for the Sn-O and Sn-Sn pairs of a TCO electrode as a function of the Li/Sn ratio during the discharge and charge cycle. Note that for a Li/Sn ratio ≤2.0, the observed coordination numbers for Sn-O/Sn-Sn pairs represent the product of the true coordination number and the mole fraction of Sn in oxidized/reduced form, respectively. For the Sn-O pair, the true coordination number is that of the pristine state (*i.e.*, prior to Li insertion), which is near 3.3. For the Sn-Sn pair, the true coordination number is the observed coordination at Li/Sn ratio of 2.0. The mole fraction for metallic Sn, as a function of the Li/Sn ratio in the range 0-2.0, can also be calculated from the observed and true coordination numbers for the Sn-O pair. The sum of the mole fractions for oxidized and reduced Sn should always add up to 1.0.

metallic Sn and Li_2O. This conclusion is in agreement with earlier results obtained on the basis of an *in situ* XRD study on crystalline Sn oxide materials.[2]

The Sn-Sn contribution could only be detected in the FT data at a Li/Sn ratio greater than 0.64, indicating that below this ratio metallic Sn is present in the TCO matrix either atomically dispersed or in a highly disordered form. The data in Fig. 5, 6, 7, and 8 can be interpreted on the basis of the corresponding electrochemical charge-discharge profiles. Hence, in region I of the electrochemical discharge profile for Li/Sn ratios in the range 1-1.6, the Sn-Sn distances are in the range 2.93-2.94 Å. These distances are intermediate to those of white Sn (4 Sn and 3.02 Å, 2 Sn and 3.18 Å) and gray Sn (4 Sn and

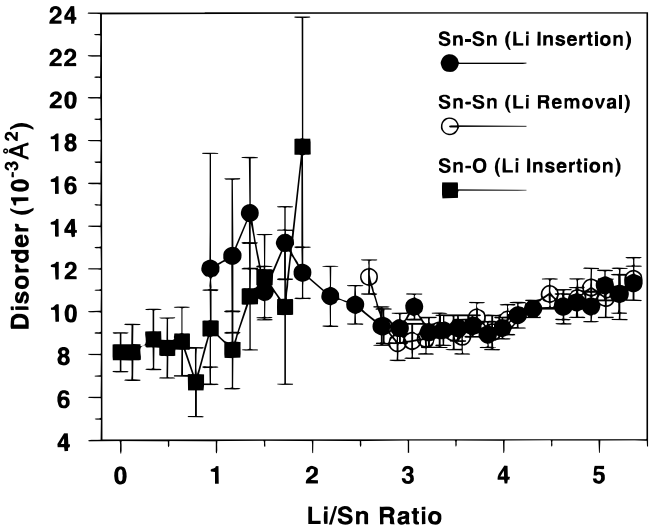

Figure 8. Variations in the disorders of the Sn-O and Sn-Sn pairs for a TCO electrode as a function of the Li/Sn ratio during the discharge and charge cycle.

2.81 Å). The Sn-Sn coordination number increased with increases in the Li/Sn ratio reaching a value of ~2 at a Li/Sn ratio near 2 during region II of the electrochemical discharge profile. Here again, up to a Li/Sn ratio <2.0, the reported coordination number for the Sn-Sn pair represents the product of the true coordination number for the Sn-Sn aggregates and the mole fraction of Sn being reduced. Thus, the increase in the reported coordination number with increases in the value of the Li/Sn ratio up to 2.0 primarily reflects an increase in the mole fraction of metallic Sn. Metallic Sn is formed as a result of the Li reaction with the electrochemically active Sn-O center and the irreversible formation of the Li_2O matrix. A comparison of the XANES data of Sn in TCO near a Li/Sn ratio of 2.0 with that of metallic white Sn confirms the formation of metallic Sn. [11] At this point, the reduction of the electrochemically active Sn-O center is complete and all the Sn is present in metallic form. The Sn-Sn coordination number of 2 at a Li/Sn ratio near 2.0, however, is still significantly less than that of white Sn, indicating that Sn is still present in a highly dispersed form. That is, Sn is present in clusters containing just a few atoms. In this case, deviation from local structure parameters for crystalline Sn is not a surprise.

Upon going from a Li/Sn ratio of 2.0 to 3.0, the end of region II, the Sn-Sn distance decreased with increases in the value of the Li/Sn ratio reaching a minimum near 2.89 Å at a Li/Sn ratio of 3.0. In this range of Li/Sn ratio, the formation of initially Li_2Sn_5 and then LiSn is expected. The XANES data show that the energy of the Sn K-edge absorption shifts continually to higher energies as the Li/Sn ratio increases from 2. to 5.4, suggesting a perturbation in the local structure of Sn. [11] This perturbation in the local structure of Sn could be due to the formation of Li_2Sn_5 and LiSn alloys proposed earlier by Courtney and Dahn.[2] However, the observed Sn-Sn distances in the Li/Sn ratio range of 2.0-3.0 are still significantly lower than those of crystalline Li_2Sn_5 and LiSn. The average Sn-Sn distance in these two alloys is near 3.14 Å, [12,13] which is slightly larger than the reported average distance of 3.08 Å for white Sn. On the basis of these results, the formation of Li_2Sn_5 and LiSn alloys must be in a highly dispersed form, as is the case for metallic Sn. Furthermore, since the local structure of Sn for Li/Sn ratios in the range 2-3 is not significantly perturbed from that of metallic Sn formed for Li/Sn ratios less than 2, the possibility of Li adsorption cannot be ruled out as a mechanism for Li interaction with metallic Sn.

In region III of the electrochemical discharge profile, the Sn-Sn distance increased from 2.89 to 2.92 Å for Li/Sn ratios in the range 3.0-5.4. In this region, the formation of at least one of four alloy phases, namely, Li_7Sn_3, Li_5Sn_2, $Li_{13}Sn_5$, and Li_7Sn_2, is expected depending on the value of the Li/Sn ratio. The Sn-Sn distance of 2.92 Å observed at a Li/Sn ratio of 5.4 is slightly smaller than that for Li_7Sn_3 (2.94 Å)[14] or Li_7Sn_2 (3.00 Å)[15] and only slightly larger than that for Li_5Sn_2 (2.88 Å)[16] or $Li_{13}Sn_5$ (2.86 Å).[17] The observed coordination number of 1.7 ± 0.2 at a Li/Sn ratio of 5.4 is closer to that of Li_7Sn_3 (N = 1.3) than those characteristic of Li_5Sn_2 (N = 1.0), $Li_{13}Sn_5$ (N = 0.8), or Li_7Sn_2 (0.5), suggesting that the formation of Li_7Sn_3 occurs near a Li/Sn ratio of 5.4. However, this phase does not account for the total amount of Li inserted. The discrepancies in the observed coordination numbers and distances for the Sn-Sn pair from those reported for known crystalline phases may be due to the formation of highly dispersed Li_xSn alloys where x depends on the value of Li/Sn ratio. These results provide evidence that the structural nature of the formed Li_xSn alloys differs significantly from those of known crystalline phases.

Upon charging (*i.e.*, Li deintercalation), the local structure parameters such as bond distance, coordination number, and disorder for the Sn-Sn interaction show reversibility with respect to corresponding values in the discharge profile (Fig. 6, 7, and 8). This corresponds to regions II and III in the electrochemical discharge profile (Fig. 1). The two regions of the charge profile corresponding to Li/Sn ratios of 5.4-3.0 and 3.0-2.3 are clear manifestations of an alloy-dealloying process. Region III (Li/Sn ratio of 5.4-3.0) is primarily a dealloying step followed by some ordering in region II by the Sn aggregates. In the fully charged state where only metallic Sn

S0013-4651(99)04-108-5 CCC: $7.00

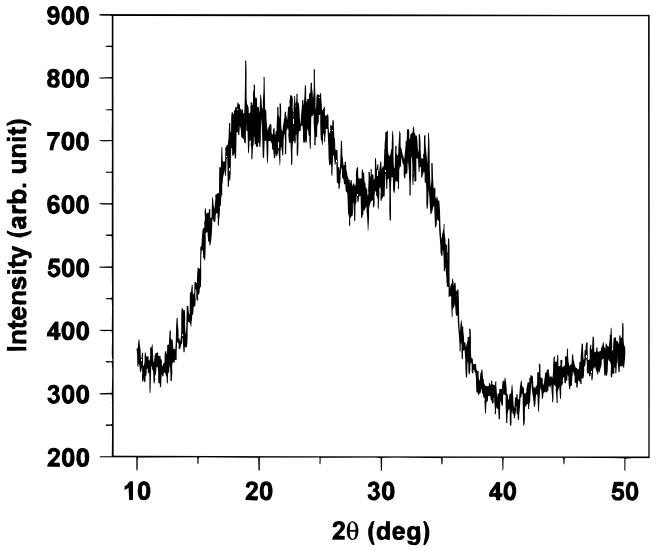

Figure 9. XRD curve for a TCO electrode taken at the end of the second charge cycle where metallic Sn is expected to form.

is expected to form, the Sn-Sn distance is 2.90 Å, which is close to that observed during the initial stages of the discharge process. A coordination number of 2.5 ± 0.3 was observed in contrast to 6 (4 at 3.02 Å and 2 at 3.18 Å) for white Sn and 4 (at 2.81 Å) for gray Sn. The lower coordination number for metallic Sn, formed as a result of Li removal, is again due to the highly dispersed nature of the Sn particles. The structure parameters in the charge step once again emphasize the irreversibility of the formation of the Li_2O matrix, which may be the key to subsequent cycling stability by enabling the Sn aggregates to remain dispersed.

The highly dispersed nature of the Sn-Sn aggregates has been confirmed by XRD. In Fig. 9, we show the XRD curve taken at the end of the second cycle of charging where metallic Sn is formed. Clearly, this curve shows a number of extremely broad bands characteristic of amorphous phases. The XRD data provide no evidence for the formation of Sn-Sn aggregates with a size large enough to be detected by XRD. The particle size for the Sn-Sn aggregates must be less than 40 Å. On the basis of the coordination numbers extracted from the XAFS spectra and assuming the shape of the particles to be spherical or cubic, the average particle size is estimated to be less than 10 Å.

Discussion and Conclusions

This investigation provides direct spectroscopic evidence for the initial electrochemical reduction of the Sn-O active center and the irreversible formation of metallic Sn during the first discharge step of a TCO glassy material. It also clearly points to an aggregation of Sn-Sn, as evidenced from an increase in the coordination number during the first stages of the discharge profile. Subsequent interaction of Li with Sn during the discharge cycle strongly indicates formation of highly dispersed clusters of Li_xSn alloys, where x depends on the degree of Li inserted. The structure of these highly dispersed alloys differs from that of known crystalline phases of Li-Sn alloys such as Li_2Sn_5, LiSn, Li_7Sn_3, Li_5Sn_2, $Li_{13}Sn_5$, and Li_7Sn_2. In an overall sense, this confirms earlier studies on crystalline SnO, SnO_2, and Sn_2BPO_6 materials by Courtney and Dahn.[2] The ability of Sn to form nanophase alloys with Li in a reversible manner has been recently reported by Mao *et al.*[18] using *in situ* Fe^{57} Mossbauer spectra in investigations of the Sn_2Fe system. Direct imaging using high-resolution transmission electron microscopy (HRTEM)[19] on nanoscale SnO anodes has also shown formation of Li-Sn alloys together with the Li_2O matrix. Hence, the initial interaction of Li with Sn in these glassy material is similar to those suggested for crystalline Sn oxides. In region I of the electrochemical discharge profile, the Li interaction with TCO glasses can be described by the following reaction

$$2Li + SnO{:}0.56B_2O_3{:}0.42P_2O_5{:}0.42Al_2O_3 \rightarrow Sn + Li_2O + 0.56B_2O_3{:}0.42P_2O_5{:}0.42Al_2O_3$$

In regions II and III, the Li interaction with TCO glasses can be described by the following reaction

$$xLi + Sn + Li_2O + 0.56B_2O_3{:}0.42P_2O_5{:}0.42Al_2 \rightarrow Li_xSn + Li_2O + 0.56B_2O_3{:}0.42P_2O_5{:}0.42Al_2O_3$$

where x is the mole fraction of Li reacting with metallic Sn. Our XAS and XRD results show that both the Sn aggregates and the Li_xSn alloys are in the form of highly dispersed clusters with a particle size less than 10 Å. Further investigations are in progress to elucidate the effect of the Sn-Sn short-range atomic order variations for these electrodes after several cycles and as a function of different depths of charge and discharge.

Acknowledgment

The authors acknowledge financial support by the Office of Naval Research, Chemistry Division, under contract no. N0001496WX20162 and the NLPP Program of NSWCCD (A.N.M.), and the USDOE, Office of Transportation Technologies (S.M., X.Q.Y., J.McB.). The support of the U.S. Department of Energy, Division of Materials Sciences, under contract no. DE-AS05-80-ER-10742, for its role in the development and operation of beam line X-11A at the National Synchrotron Light Source (NSLS) is also acknowledged. The NSLS is supported by the Department of Energy, Division of Materials Sciences and Division of Chemical Sciences, under contract no. DE-AC02-76CH00016.

The U.S. Naval Surface Warfare Center assisted in meeting the publication costs of this article.

References

1. Y. Idota, T. Kubota, A. Matsufuji, Y. Maekawa, and T. Miyasaka, *Science*, **276,** 1395 (1997).
2. I. A. Courtney and J. R. Dahn, *J. Electrochem. Soc.*, **144,** 2943 (1997).
3. I. A. Courtney and J. R. Dahn, *J. Electrochem. Soc.*, **144,** 2045 (1997).
4. S. Machill, T. Shodia, Y. Sakurai, and J.-I. Yamaki, *J. Power Sources*, **73,** 215 (1998).
5. S. C. Nam, Y. H. Kim, W. I. Cho, B. W. Cho, H. S. Chun, and K. S. Yun, *Electrochem. Solid-State Lett.*, **2,** 9 (1999).
6. Y. Idota, M. Mishima, Y. Miyaki, T. Kubota, and T. Miyasaka, European Pat. 65,145,0A1 (1995).
7. J. McBreen, S. Mukerjee, X. Q. Yang, T. R. Thurston, and N. M. Jisrawi, in *Proceedings of the 2nd International Symposium on New Materials and Modern Battery Systems*, O. Savadogo and R. Roberge, Editors, p. 348, Ecole Polytechnique, Montreal, Canada, July 6-10,1997.
8. S. I. Zabinsky, J. J. Rehr, A. Ankudinov, R. C. Albers, and M. J. Eller, *Phys. Rev. B*, **52,** 2995 (1995).
9. E. A. Stern, M. Newville, B. Ravel, Y. Yacoby, and D. Haskel, *Physica B*, **208&209,** 117 (1995).
10. P. Villars and L. D. Calver, *Pearson's Handbook of Crystallographic Data for Intermetallic Phases*, Vol. 3, p. 2730, American Society for Metals, Metals Park, OH (1985).
11. A. N. Mansour, S. Mukerjee, X.-Q. Yang, and J. McBreen, *J. Synchrotron Radiation*, **6,** 596 (1999).
12. D. A. Hansen and L. J. Chang, *Acta Crystallogr. B*, **25,** 2392 (1969).
13. W. Muller and H. Schafer, *Z. Naturforsch.*, **28b,** 246 (1973).
14. W. Muller, *Z. Naturforsch.*, **29b,** 304 (1974).
15. U. Frank, W. Muller, and H. Schafer, *Z. Naturforsch.*, **30b,** 6 (1975).
16. U. Frank, W. Muller, and H. Schafer, *Z. Naturforsch.*, **30b,** 1 (1975)
17. U. Frank and W. Muller, *Z. Naturforsch.*, **30b,** 316 (1975).
18. O. Mao, R. A. Dunlup, I. A. Courtney, and J. Dahn, *J. Electrochem. Soc.*, **145,** 4195 (1998).
19. H. Li, X. Huang, and L. Chen, *Electrochem. Solid-State Lett.*, **1,** 241 (1998).